

Configuration of vortex-antivortex lattices at output mirror of wide-area microchip laser

A.Yu.Okulov*

Russian Academy of Sciences, 119991, Moscow, Russia

(Dated: November 2, 2018)

Square vortex lattices predicted theoretically and experimentally observed in diode-pumped solid state microchip lasers are shown to have a remarkable symmetry. These lattices are formed by counter-rotating vortices. The interaction of vortices with nonlinear gain medium leads to precession of vortices and collective excitations with dynamics identical to acoustical and optical vibrations of atomic lattices.

PACS numbers: 42.65.Hw, 42.65.Jx, 42.65.Re, 42.55.Wd, 42.60.Jf

I. INTRODUCTION

Pattern formation outside the equilibrium demonstrates a rich variety of emerging structures [1, 2]. The vortex lattices in high Fresnel number solid-state microchip lasers arising within a broad range of experimental parameters [3] were predicted theoretically in [4]. The subsequent numerical investigation [5] have shown the deep similarity of optical vortex lattices in lasers with spatial patterns that spontaneously occur in Faraday instability [6]. Trajectories of individual particles of ensemble in Faraday convection are chaotic but the averaged mass flow in Faraday square cells manifests itself as vortex lattice. The elementary cell consists from a four vortices. Each pair of whirls located at the corners of the cell are co-rotating and each pair of adjacent whirls at the side of the cell are counter-rotating. The corresponding field of velocities averaged over ensemble of particles is continuous though each given particle in ensemble moves on complex trajectory [6].

The same patterns were observed in wide area diode-pumped solid state microchip lasers [7]. The Fresnel number N_f in these experiments had been varied from 10 to 1000, the number of synchronously counter-rotating vortices along the side of the square was about $N_L = 30$. The spatially periodic vortex-antivortex patterns recorded experimentally in a broad range of system parameters are in remarkable difference from conventional sets of Gaussian-Hermite (HG) or Gaussian-Laguerre (LG) eigenmodes. The square pattern occurs due to phase-locking of HG or LG modes via nonlinearity inherent to gain medium [8]. The theoretical study in [4] and subsequent experimental confirmation [3] overlooked the phase structure of optical field $\theta(\vec{r}) = \arg[E_n(\vec{r})]$. The investigation of spatial phase distribution of optical field and associated probability flow with appropriate field of velocities $\vec{v}(\vec{r}) = \hbar \nabla \theta(\vec{r}) / m$ given by Madelung transform have shown the existence of regular array of whirls with opposite circulations [9]. Current survey is aimed

to study nonstationary regimes of vortex-antivortex lattices formation when stationary solutions are perturbed by noise sources due to spontaneous emission $\delta E_n(\vec{r})$ and fluctuations of optical pump $\delta N_n(\vec{r})$.

II. MASTER EQUATION AND OBSERVED DYNAMICS

The master equation for the square lattice pattern formation is of Ginzburg-Landau type [10]. The other model relevant to laser cavity under consideration is equivalent to Fox-Lee integral with nonlinear gain included in explicit form [11]:

$$E_{n+1}(\vec{r}) = \int \int_{-\infty}^{\infty} K(\vec{r} - \vec{r}') f(E_n(\vec{r}')) d^2 r', \quad (1)$$

$$K(\vec{r} - \vec{r}') = \frac{ikD(\vec{r}')}{2\pi L_r} \exp[ik(\vec{r} - \vec{r}')^2 / 2L_r]. \quad (2)$$

$$f(E_n(\vec{r})) = \frac{\sigma L_a N_n(\vec{r}) E_n(\vec{r}) (1 + i\delta\omega T_2)}{2 E_n(\vec{r}) + \delta E_n(\vec{r})}, \quad (3)$$

inversion dynamics is given by:

$$N_{n+1}(\vec{r}) = N_n(\vec{r}) + \left[\frac{N_0(\vec{r}) - N_n(\vec{r}) + \delta N_n(\vec{r})}{T_1} - \sigma N_n(\vec{r}) c_{\epsilon_0} |E_n|^2 / \hbar\omega \right] \frac{2L_r}{c}, \quad (4)$$

where $E_n(\vec{r})$ is electric field envelope at output mirror, f is nonlinear gain transfer function, L_r is cavity length, $L_a \ll L_r$ is a thickness of amplifying medium relevant to experimental situation [12], R is reflectivity of output mirror, $D(\vec{r}) = R \exp[-|\vec{r}|^2 / D_0^2]$ is diaphragm function corresponding to transversely inhomogeneous linear losses, key parameter for comparison with experiments [3] was $D_0 \sim 50 - 2000 \mu\text{m}$, $G_n(\vec{r}) = \sigma N_n(\vec{r}) L_a$ is transversely inhomogeneous linear gain, σ is simulated emission cross-section, $N_n(\vec{r})$ is density of resonant ions per unit volume, $\delta\omega$ is detuning from gain line

*Electronic address: alexey.okulov@gmail.com;
URL: <https://sites.google.com/site/okulovalexey>

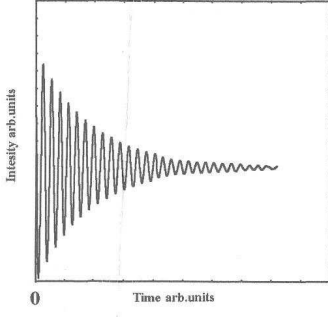


FIG. 1: Temporal evolution of intensity $|E_n(\vec{r})|^2$ under stepwise gain switching.

center, T_2 and T_1 are transverse and longitudinal relaxation times correspondingly, $\delta E(\vec{r})$ is random noise due to spontaneous emission term emulated as multimode random process [13], $\delta N(\vec{r})$ is fluctuating part of optical pump also defined as spatially smooth multimode random process, $N_f = D_0^2/(\lambda L_r)$ is Fresnel number, λ is lasing wavelength. The convergence rate to equilibrium solutions (stationary eigenmodes) for discrete time step $\delta t = 2L_r n/c$ proved to be 20 - 100 iterates [14].

For modeling of nonstationary behavior approximately the same amount of transient iterates had been required [15] to attain a realistic oscillation regime with smooth spatial field profile $E_n(\vec{r})$. The most reliable convergence to realistic solutions had been observed for relaxation oscillations (fig.1,2). For low Fresnel number $1 < N_f < 10$ the transient behavior of numerical scheme had been pretty good realistic from the very first iterates started from completely random transverse field $E_n(\vec{r})$ taken as multimode random process with N_m spatial harmonics with random phases $\delta\phi_n$ [13]:

$$\delta E_n(\vec{r}) = N_m^{-1} \sum_m^{N_m} |A_1 + A_2 + \dots + A_m + \dots|^2 ;$$

$$A_m = \delta A_0 \exp[i\vec{k}_m \cdot \vec{r} + \delta\phi_n], \quad (5)$$

Numerical arrays $E_n(\vec{r})$ (complex) and $N_n(\vec{r})$ (real) were composed of [128,128] and [256,256] points to facilitate the usage of fast Fourier transform [15] optimized for standard Fortran compiler. In most realizations at $1 < N_f < 10$ the transverse field distribution $E_n(\vec{r})$ had been almost identical to fundamental TEM_{00} gaussian mode $E_n(\vec{r}) \sim \exp[-|\vec{r}|^2/D_0^2]$ with slightly different D_0 .

Increase of Fresnel number have led to perpetual increase of complexity of output pattern. In most cases for $10 < N_f < 50$ the stationary output resulted in selection of Hermite- Gaussian and Laguerre-Gaussian functions. All these low-order eigenfunctions of **2D** of harmonic oscillator [16, 17] were also subjected to relaxation oscillations (fig.3) due to intermediate value of cavity lifetime τ_c :

$$T_1 < \tau_c < T_2, \quad \tau_c = 2L_r n/(c(1 - R)), \quad (6)$$

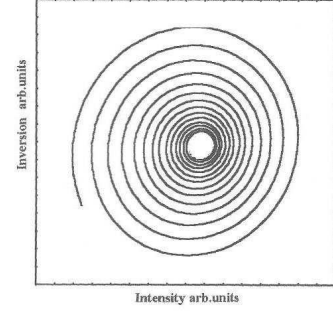


FIG. 2: Temporal evolution in phase-space of intensity $|E_n(\vec{r})|^2$ and inversion N_n under stepwise gain switching.

The characteristic frequency ω_{rel} for observed relaxation oscillations was close to:

$$\omega_{rel} \sim \sqrt{T_1 \tau_c} \sqrt{G - 1}; \quad G = \sigma N_0(\vec{r} = 0). \quad (7)$$

In a parameter region between $8 < N_f < 50$ and $1.5 < G - 1 < 3$ a certain realizations on initial conditions $\delta E_n(\vec{r})$ have led to localized excitations close to dissipative solitons [11, 18] of **2D** hyperbolic secant profile [19, 20].

III. SINGULAR LATTICES AND THEIR VIBRATIONS

The stationary patterns at higher Fresnel numbers $10^2 < N_f < 10^3$ demonstrated a remarkable phase locking phenomena. The synchronized modes of empty resonator form an almost perfect periodic lattice of dark spots [9]. Each dark spot is surrounded by a nearly circular flow resembling isolated optical vortex alike Laguerre-Gaussian beam [21, 22]. The phase of optical field is a precise indicator of electromagnetic energy circulation [23]. When phase is increased from 0 to 2π along right-handed circular path around amplitude $E_n(\vec{r})$ zeros, the azimuthal flow of probability to find photon in a given volume is accompanied by right-handed azimuthal component of Pointing vector $\vec{S} = \epsilon_0 c^2 \vec{E} \times \vec{H}$ [9]. The swirling of electromagnetic energy is counter-clockwise in opposite case of left-handed probability flow (fig.5). A part of numerically obtained patterns is composed from zeros of amplitudes equispaced in a checkerboard geometry with alternating circulations as is shown in [8]. The macroscopic photons wavefunction $\Psi \sim E_n(\vec{r})$ [21] which is visualized by electric field amplitude $E_n(\vec{r})$, demonstrates the regular lattices of field zeros with counter-rotating whirls around [fig.6]. In contrast to optical speckle patterns [24] where vortex-antivortex pairs are distributed chaotically in space the lattice of whirls in wide-aperture lasers is periodic in space [fig.5]. The far field pattern consists of four lobes whose separation is defined by wavelength λ and period p of the near field pattern [5].

The other set of numerical realizations appears to

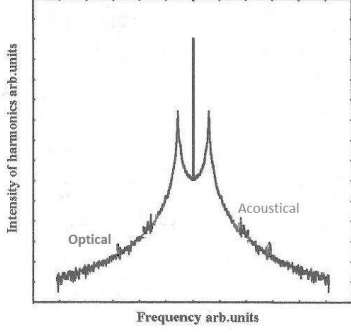


FIG. 3: The power spectrum of wide area (high Fresnel number $100 < N_F < 1000$) stationary emission perturbed by spontaneous noise added at each round trip n . Noteworthy the collective excitations spikes interpreted as acoustical and optical vibrations of vortex lattice of 9×9 whirls.

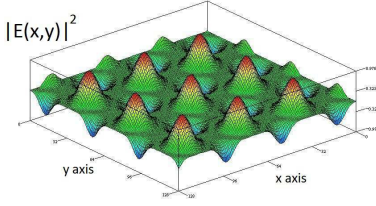


FIG. 4: The stationary transverse intensity distribution $|E_n(\vec{r})|^2$ of wide area laser stationary emission with high Fresnel number $100 < N_F < 1000$.

be identical to Abrikosov lattice obtained analytically $\Psi \sim \vartheta_3[\sqrt{2\pi i\kappa}(x + iy); 1]$ [25], where κ is ratio of coherence length to penetration depth, ϑ_3 is Jacobi theta function (fig.4). Exactly as in the early models of type-II superconductors placed in external magnetic field [25] the vortices at zeros of amplitudes have co-directed angular momenta but the field of velocities is continuous as well due to rotation around bright spots. The energy flow around maxima of intensity is opposite to flow around zeros. Both types of vortex lattices obtained numerically have remarkable square symmetry found yet in [25]. Noteworthy experimentally observed lattices in superconductors of the second type have triangular symmetry.

The noise sources due to spontaneous emission $\delta E_n(\vec{r})$ and fluctuations of optical pump $\delta N_n(\vec{r})$ have led to vibrations of vortex lattices. To detect vibrations the power spectrum $I(\Omega) = FFT[|E_n(\vec{r})|^2]$ had been recorded at several points \vec{r} of transverse section. In the stationary regime with well formed vortex lattice the spectrum $I(\Omega)$ proved to be independent of location \vec{r} . The large maximum near frequency of relaxation oscillations had been recorded in all oscillation regimes and for all transverse spatial distributions. The remarkable feature of obtained patterns are small maxima of power spectrum beyond relaxation frequency. The early numerical study reported this spikes at power spectrum as

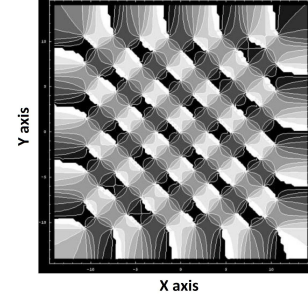


FIG. 5: The grey scale stationary transverse phase distribution $arg[E_n(\vec{r})]$ of wide area (high Fresnel number $100 < N_f < 1000$) laser. Black color corresponds to phase $arg[E_n(\vec{r})] = 0$ which gradually increases to $arg[E_n(\vec{r})] = 2\pi$ in circumvention around vortex cores.

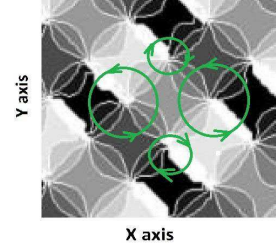


FIG. 6: The enlarged elementary cell grey scale transverse phase distribution $arg[E_n(\vec{r})]$ of wide area (high Fresnel number $100 < N_f < 1000$) laser nonstationary emission.

collective vibrations of vortex lattice [4]. The mechanism responsible for lattices vibrations had been reported as vortex precession around equilibrium position. In our numerical model the observed vortex lattices of 4×4 , 7×7 and 9×9 whirls were practically unmovable at a long discrete time n intervals. Nevertheless the sufficiently large vortex lattice composed of 9×9 whirls produced numerical noise spectrum with a small but clearly visible collective excitation spikes (fig.3). As is known from lattice vibration theory there exist two basic types of collective lattice vibrations with a different dispersion laws. The acoustic mode corresponds to running waves whose group velocity tends to zero at the edge of the first Brillouin zone. The optical mode of vibrations possesses the higher frequencies with significantly smaller group velocities. The discrete time n to record this spectrum $I(\Omega)$ was about 500 time steps (iterates of maps(1-4)). The runtime took for about a one minute on *dual core* 1.86Ghz processor per each FFT accelerated iteration of discrete master equations (1-4).

IV. CONCLUSION

The computational model for eigenmodes $E_n(\vec{r})$ of microchip laser resonator is composed of convolution integral with nonlinear kernel evaluated via Fast-Fourier

transform [11, 14] and the relaxation oscillator $N_n(\vec{r})$ for gain medium coupled with wavefunction $E_n(\vec{r})$. The regular square lattices (fig.4,5) appear in a well defined range of key system parameters namely laser gain and Fresnel

number. The inherent feature of these nonstationary vortex patterns are vibrations of observed lattices which are known as optical and acoustical ones (fig.3).

-
- [1] Cross M. C. and Hohenberg P. C. 1993 Pattern formation outside of equilibrium *Rev. Mod. Phys.*, **65**, 851
 - [2] Okulov A.Yu. and Oraevsky A.N. 1986 Spatio-temporal behavior of a light pulse in nonlinear nondispersive media *J. Opt. Soc. Am B* **3** 741
 - [3] Chen Y. F. and Lan Y. P. 2001 Transverse pattern formation of optical vortices in a microchip laser with a large Fresnel number *Phys. Rev. A* **65**, 013802
 - [4] K.Staliunas and C.O.Weiss 1995 Nonstationary vortex lattices in large-aperture class B lasers *J. Opt. Soc. Am B* **12**, 1142
 - [5] Okulov A.Yu. 2008 3D-vortex labyrinths in the near field of solid-state microchip laser *J. Mod. Opt.* **55**, 241-259
 - [6] Francois N., Xia H., Punzmann H., Ramsden S. and Shats M., 2014 Three-dimensional fluid motion in Faraday waves: creation of vorticity and generation of two-dimensional turbulence *Phys. Rev. X* **4**, 021021
 - [7] Chen Y. F. and Lan Y. P. 2003 Observation of transverse patterns in an isotropic microchip laser *Phys. Rev. A*, **67**(4), 043814
 - [8] Okulov A.Yu. 2004 3D-configuration of the vortex lattices in microchip laser cavity QCMC-2004, *AIP Conference Proceedings* **734**, p.366
 - [9] Okulov A.Yu. 2009 Vortex-antivortex wavefunction of a degenerate quantum gas *Laser Physics* **19**, 1796-1803
 - [10] Burlak G. and Malomed B.A. 2018 Interactions of three-dimensional solitons in the cubic-quintic model *Chaos* **28**, 063121
 - [11] Okulov A.Yu. and Oraevsky A.N. 1988 Spatiotemporal dynamics of a wave packet in nonlinear medium and discrete maps, *Proceedings Lebedev Physics Institute (in Russian)* N.G.Basov ed., Nauka, Moscow **187**, 202-222
 - [12] Vadimova O.L., Mukhin I.B., Kuznetsov I.I., Palashov O.V., Perevezentsev E.A. and Khazanov E. A. 2013 Calculation of the gain coefficient in cryogenically cooled Yb : YAG disks at high heat generation rates *Quantum Electronics* **43**, n.3, 201-206
 - [13] Okulov A.Yu. 1991 The effect of roughness of optical elements on the transverse structure of a light field in a nonlinear Talbot cavity *J. Mod. Opt.* **38**, n.10, 1887
 - [14] Okulov A.Yu. 1994 On correlations between cavity mode and inversion profile in a solid-state microchip laser *Optics and Spectroscopy* **77**, n.6, 888-892
 - [15] Okulov A.Yu. 1993 Scaling of diode-array-pumped solid-state lasers via self-imaging *Opt. Comm.* **99**, p.350-354
 - [16] Chen Y. F. and Lan Y. P., 2002 Observation of laser transverse modes analogous to a SU(2) wave packet of a quantum harmonic oscillator *Phys. Rev. A* **66**(5), 053812
 - [17] Chen Y. F., Hsieh Y. H., and Huang K. F. 2018 Originating an integral formula and using the quantum Fourier transform to decompose the Hermite-Laguerre-Gaussian modes into elliptical orbital modes *OSA Continuum*, **1**, Issue 2, pp. 744-754
 - [18] Okulov A.Yu. 2000 Spatial soliton laser: geometry and stability *Optics and Spectroscopy* **89**, 145-147
 - [19] Okulov A.Yu. 2004 Exact theory of localized and periodic structures in an active optical resonator *Bulletin of Lebedev Physical institute*, n.10
 - [20] Malomed B.A. and Towers I. 2002 Stable (2+ 1)-dimensional solitons in a layered medium with sign-alternating Kerr nonlinearity *J. Opt. Soc. Am B* **19** 537-543
 - [21] Okulov A.Yu. 2012 Rotational Doppler shift of the phase-conjugated photons, *J. Opt. Soc. Am B* **29**, 714-718
 - [22] Rashed A. Al, Lyras A., Lembessis V. E., Aldossary O. M. 2016 Guiding of atoms in helical optical potential structures *J. Phys. B* **49** 125002
 - [23] Rashed A. Al, Lyras A., Lembessis V. E., Alqarni A., Alshamari S., Siddig A., Aldossary O. M. 2016 Rotating optical tubes for vertical transport of atoms *Phys. Rev. A* **94**, 063423
 - [24] Okulov A.Yu. 2009 Twisted speckle entities inside wave-front reversal mirrors *Phys. Rev. A* **80**, 013837
 - [25] Abrikosov A.A. 1957 On the magnetic properties of superconductors of the second group *JETP* **5** 1174